

# **An Experimental and Statistical Study of Normal Strength Concrete (NSC) to Ultra High Performance Concrete (UHPC) Interface Shear Behavior**

**Sumedh Sharma** – PhD Student, 2024 SERC Building, Dept. of Civil, Const. & Env. Engineering, University of Alabama, Tuscaloosa, AL 35487 USA, Phone: 205-764-7659, Email: [ssharma11@crimson.ua.edu](mailto:ssharma11@crimson.ua.edu)

**Sriram Aaleti, Ph.D.** \* (corresponding author) – Asst. Professor, 2037C SERC Building, Dept. of Civil, Const. & Env. Engineering, University of Alabama, Tuscaloosa, AL 35487 USA, Phone: 205-348-0783, Email: [saaleti@eng.ua.edu](mailto:saaleti@eng.ua.edu)

**Thang N. Dao, Ph.D.** – Asst. Professor, 2037A SERC Building, Dept. of Civil, Const. & Env. Engineering, University of Alabama, Tuscaloosa, AL 35487 USA, Phone: 205-348-0726, Email: [tndao@eng.ua.edu](mailto:tndao@eng.ua.edu)

## **Abstract:**

With number of existing bridges in U.S, classified as structurally deficient and many bridges nearing end of their design service life, there is a need for a durable and accelerated construction solution. Recently, several state DOTs developed innovative solutions using Ultra-High Performance Concrete (UHPC) as infill material between prefabricated bridge components or as an overlay over existing structural elements. The normal strength concrete (NSC) to UHPC interface behavior is critical for overall performance of such structures. Experimental investigation consisting of 10 push-off specimens was performed to investigate shear transfer behavior at NSC-UHPC interface. In general, the results showed that increasing roughness depth and reinforcement area has positive effect in interface shear capacity. The experimental results were compared with current AASHTO LRFD, ACI and PCI design guidelines. Though the design guidelines were conservative; they were not accurate in predicting the interface shear strength. Additionally, a database including results from past push-off tests on NSC-UHPC interface was developed and a reliability analysis was carried out with respect to AASHTO LRFD design guidelines. The reliability index was found to be lower than the target reliability index in standard design practices.

**Keywords:** NSC-UHPC interface, design equation, Accelerated Bridge Construction, reliability analysis

## **1. Introduction**

As of 2016, nearly 9.1 % of the bridges in the United States were classified as structurally deficient, with the average age of the bridges reaching 43 years. Almost 39% of bridges were past design service life of 50 years, and 10% of total bridges had certain weight or speed restriction. The structurally deficient bridges themselves were subjected on average 188 million trips each day (ASCE 2017). These bridge infrastructure challenges point towards need of robust and durable rehabilitation methods for structurally deficient bridges and innovative accelerated bridge construction (ABC) practices for shorter construction time. These advancements are also necessary to address increased emphasis on work zone safety, users cost associated with traffic delays, and the environmental impacts of the construction process (Aaleti & Sritharan 2014).

Ultra-high performance concrete (UHPC) is a new class of cementitious material, which exhibits superior mechanical and durability properties compared to normal strength concrete (NSC). In recent times, it is being used as an overlay over existing deficient concrete bridge decks and as a field-cast closure pour or grout material in connections between precast bridge components. The interface bond capacity between precast concrete and field-cast UHPC is critical in determining the overall strength and durability of such composites. The interface bond strength should be sufficient to resist any stresses developed due to mechanical and thermal loads while also maintaining an extended service-life performance (Munoz et al. 2014). The shear stress transfer mechanism between the UHPC and normal concrete layers is a complex phenomenon and is governed by different factors such as roughness of the interface, amount of reinforcement across the interface, the compression strength of the weaker concrete, and compressive stress generated by normal forces across the interface. The interface shear strength between NSC concrete layers can be calculated using different standard design equations. The applicability and reliability of those equations for predicting the NSC-UHPC interface strength is needed to be evaluated.

## 2. Background

### 2.1. Interface Shear Friction

Shear-friction theory initially developed by Birkeland and Birkeland, estimates interface shear resistance in terms of friction force across a roughened surface (Birkeland & Birkeland 1966). Shear loading causes longitudinal slip across the interface after overcoming aggregate interlock, which results in displacement in the transverse direction. This displacement causes tension force in interface steel reinforcement which creates normal clamping force across the interface. The friction force is the product of the normal clamping forces across the interface and the tangent of the contact angle across the surface. The current understanding of shear force transfer mechanism across concrete interface has evolved to include the contributions due to adhesion (chemical bonds between the particles of old and new concrete), shear friction and dowel action (Santos & Julio 2014). The existing design code equations for determining interface strength are presented in Table 1.

**Table 1 Design equations for interface shear strength in design codes**

	AASHTO LRFD 7 <sup>th</sup> ed. (5.8.4)	ACI 318-14 (22.9.4)	PCI 7 <sup>th</sup> ed. (5-32a)
Equations	$V_{ni} = cA_{cv} + \mu(A_{vf}f_y + P_c)$	$V_{ni} = \mu A_{vf}f_y$	$V_{ni} = \mu A_{vf}f_y$
Limitations	$V_{ni} \leq K_1 f'_c A_{cv}$ $V_{ni} \leq K_2 A_{cv}$ $A_{vf} \geq 0.05 A_{cv}/f_y$ and $f_y \leq 414 \text{ MPa (60 ksi)}$	For monolithic or roughened surface cases $V_{ni} \leq (3.31 + 0.08f'_c) A_{cv}$ For all the cases $V_{ni} \leq K_1 f'_c A_{cv}$ $V_{ni} \leq K_2 A_{cv}$ and $f_y \leq 414 \text{ MPa (60 ksi)}$	$V_{ni} \leq K_1 f'_c A_{cv}$ $V_{ni} \leq K_2 f'_c A_{cv}$ $f_y \leq 414 \text{ MPa (60 ksi)}$

Note:  $A_{cv}$  = area of shear interface,  $A_{vf}$  = area of interface shear reinforcement,  $P_c$  = permanent net compressive force,  $f_y$  = yield strength of interface shear reinforcement,  $\mu$  = coefficient of friction, and  $c$  = cohesion factor,  $K_1$  is fraction of concrete strength available to resist interface shear, and  $K_2$  is limiting interface shear resistance

The design codes provide different values for coefficient of friction ( $\mu$ ), cohesion factor (c), fraction of concrete strength available to resist interface shear ( $K_1$ ) and limiting interface shear resistance ( $K_2$ ) according to surface preparation at the shear interface.

## 2.2. Reliability Analysis

Structural safety is one of the major criteria of a sound engineering design. The typical load and resistance components used in structural design come with inherent uncertainties; the effects of which can be quantified using reliability analysis. A reliability analysis for typical structure problem requires definition of a ‘limit’ state function. A limit state function consists of resistance and load model.

If R represents the resistance and Q represents the load effects on a structure, the corresponding limit state function can be written as  $g(R, Q) = R - Q$  (Nowak & Collins 2000). Such structure is safe if  $g(R, Q) > 0$ . Thus, the probability of failure ( $p_f$ ) of such structure can be expressed as:  $p_f = P(g(R, Q) < 0)$ . The reliability index is related to the probability of failure as:

$$\beta = -\phi^{-1}(p_f) \quad (1)$$

If both R and Q are normally distributed, random and independent random variables, the reliability index can be determined as:

$$\beta = \frac{m_R - m_Q}{\sqrt{\sigma_R^2 + \sigma_Q^2}} \quad (2)$$

where,  $m_R$  = mean value of resistance model,  $m_Q$  = mean value of load model,  $\sigma_R$  = standard deviation of resistance model,  $\sigma_Q$  = standard deviation of load model

## 2.3. Previous NSC-UHPC Interface Shear Study

Banta (2005), Crane (2010) and Jang et al. (2017) performed push-off tests to determine the interface shear capacity relating to UHPC. Banta performed tests consisting of Light Weight Concrete (LWC)-UHPC interface; Crane performed tests consisting of High Performance Concrete (HPC)-UHPC interface and Jang et al. performed tests consisting of UHPC-UHPC and NSC-UHPC interface. Specimens with rougher interface surface preparation and higher interface reinforcement ratio performed better in terms of interface shear capacity. Banta and Crane observed near linear increment in interface shear with respect to area of interface reinforcement. Jang et al. observed that in UHPC-UHPC specimen, the distribution of steel fibers across the interface through horizontal grooves added to ductility and produced superior interface shear strength.

Sarkar (2010), Munoz et al. (2014) and Aaleti and Sritharan (2017) performed slant shear tests on NSC-UHPC composites. Sarkar observed that specimens with no surface preparation failed along the interface while specimens with surface preparation failed through the normal concrete substrate. Munoz et al. also studied the effects of interface angles on interface bond strength. The specimens with an interface angle of  $60^\circ$  failed in the concrete substrate; while the specimens with interface angle of  $70^\circ$  experienced sliding failures. Based on slant shear test results, Aaleti and Sritharan recommended a minimum roughness of 2 mm (0.08 in.) to develop adequate bond strength under combined shear and compression loads. The researchers did not find significant influence of pouring sequence on interface bond strength.

Crane, Sarkar and Aaleti and Sritharan also performed bending tests on NSC-UHPC composite flexural specimens. Crane performed tests on small-scale composite T-beam specimens made of UHPC in the web and HPC in the flanges and large scale tests on precast prestressed UHPC bridge girders with cast-in-place HPC decks. Based on the tests, Crane recommended using a fluted interface in cold-joint interface and avoid using smooth cold-joint interface. In the bending tests performed by Sarkar, Aaleti and Sritharan, shear stress ranging from 1.0 MPa (0.15 ksi) to 1.4 MPa (0.2 ksi) was observed along the NSC-UHPC interface before failure of substrate.

Previous studies have shown adequate interface shear strength between UHPC and corresponding substrate concrete material especially when adequate interface roughness was provided. But, there are limited tests on NSC-UHPC specimen with reinforcement at the interface. Jang et al. conducted push-off tests in NSC-UHPC interface but did not investigate cases with reinforcement at the interface. Banta and Crane focused on behavior of interface reinforcement in smooth interface while studying LWC-UHPC and HPC-UHPC composites. The behavior of interface reinforcement in NSC-UHPC composites with roughened interface needs to be studied in further detail. Also, the variability in the measured interface bond values warrants a reliability study to understand the safety associated with current design code equations.

### 3. Experimental Study

#### 3.1. Specimen Details and Test Setup

In the experimental study, push-off specimens with different combinations of interface roughness and shear reinforcement were used to understand their effects on interface shear capacity. Two interface textures, namely, Wisla and Parana having interface roughness of 5 mm (0.2 in.) and 2 mm (0.08 in.) respectively were selected from Reckli® formliners to obtain accurate and repeatable roughness texture. Commercial UHPC mix (Ductal®) from Lafarge was used in the study. Table 2 provides the details of different interface texture and interface reinforcement used in the push-off test specimens. The typical dimensions of the specimen are shown in Figure 1.

**Table 2 Details of push off specimen**

Specimen identification no.	Shear interface texture	Interface roughness depth mm (in.)	Interface area mm <sup>2</sup> (in <sup>2</sup> )	Area of interface shear reinforcement mm <sup>2</sup> (in <sup>2</sup> )
SM-0-A	Smooth	0.00 (0.00)	40,129 (62.2)	0.00 (0.00)
SM-0-B	Smooth	0.00 (0.00)	41,581(64.45)	0.00 (0.00)
PI-0	Parana	2.03 (0.08)	40,284 (62.44)	0.00 (0.00)
WI-0	Wisla	5.08 (0.2)	41,084 (63.68)	0.00 (0.00)
SM-1-A	Smooth	0.00 (0.00)	41,129 (63.75)	142 (0.22)
SM-1-B	Smooth	0.00 (0.00)	42,678 (66.15)	142 (0.22)
PI-1	Parana	2.03 (0.08)	41,458 (64.26)	142 (0.22)
WI-1	Wisla	5.08 (0.2)	39,632 (61.43)	142 (0.22)
PI-2	Parana	2.03 (0.08)	43,671 (67.69)	284 (0.44)
WI-2	Wisla	5.08 (0.2)	40,522(62.81)	284 (0.44)

The push-off specimens were tested using 890 kN (200 kips) capacity hydraulic jack. A non-contact measurement system (Optotak system) was used to measure interface slip and dilation of the interface. Typically, four pairs of Light Emitting Diodes (LEDs) equally spaced apart were installed across NSC-UHPC interface as shown in Figure 1a. The Optotak system recorded 3D coordinates of the LEDs at a rate of 10 Hz. Strain gauges installed at three locations

along the interface reinforcement were used to monitor the strains and force development in the reinforcement. The locations of the strain gauges are shown in Figure 1b. The load data was recorded using a 445 kN (100 kip) load cell. The data from all the instruments was recorded using National Instruments (NI) Data Acquisition System (DAQ) system. The load was applied monotonically in increments of 11 kN (2.5 kip) up to failure of the specimen.

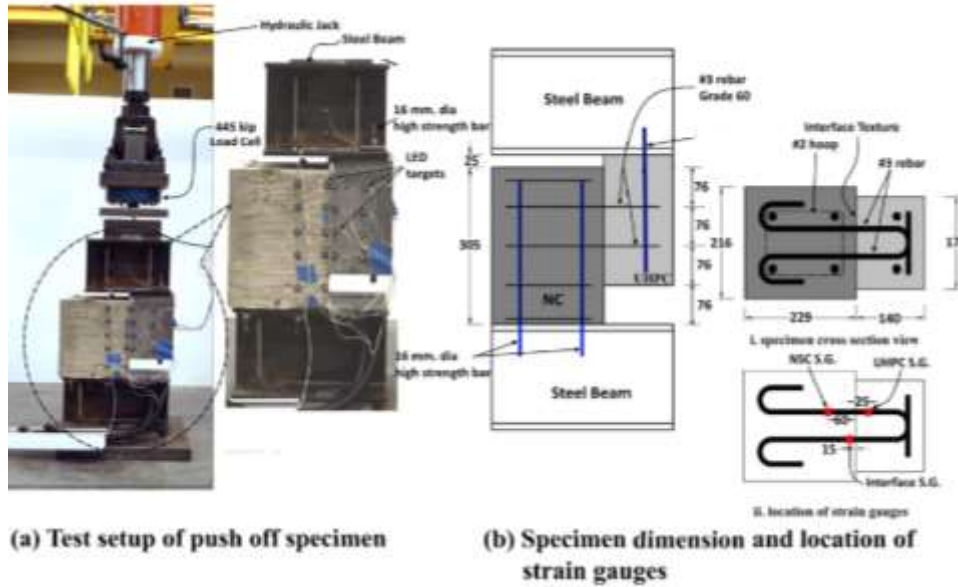


Figure 1 Test setup and specimen detail for push off specimen

### 3.2. Results and Discussion

The measured average compressive strength ( $f'_c$ ) of UHPC and NSC was 45 MPa (6.53 ksi) and 123.23 MPa (17.88 ksi) respectively. The results from the push off test in terms of cracking load; peak load; slip and dilation in the interface; and strain in interface reinforcement are presented in Table 3. Figure 2 shows force vs slip relationship of the tested specimens. The slip in Figure 2 was limited to 0.4 in. for proper presentation of data. Specimen (SM-0-B) failed due to accidental loading and thus was removed from analysis. As expected, the specimens with higher interface roughness such as Parana (PI: 2 mm) and Wisla (WI: 5 mm) performed better than smooth (SM) specimens. Specimens with same interface roughness but with increased area of interface reinforcement resisted higher shear.

Table 3 Results from Push-off tests

Specimen identification no.	Cracking load <sup>a</sup> kN (kip)	Peak load kN (kip)	Slip <sup>b</sup> mm.(in.)	Crack width <sup>b</sup> mm. (in.)	Strain in interface reinforcement <sup>b</sup>	Shear stress MPa (ksi)
SM-0-A	N/A	45.0(10.1)	0.33(0.01)	N/A	N/A	1.10(0.16)
SM-0-B	N/A	6.00(1.35)	N/A	N/A	N/A	0.14(0.02)
PI-0	N/A	62.2(14.0)	0.33(0.01)	1.52(0.06)	N/A	1.52(0.22)
WI-0	N/A	137.6(30.9)	0.28(0.01)	0.04(0.002)	N/A	3.38(0.49)
SM-1-A	82.6(18.6)	116.9(26.3)	40.38(1.59)	10.67(0.42)	0.0080	2.83(0.41)
SM-1-B	7.1(1.6)	111.2(25.0)	10.67(0.42)	2.79(0.11)	0.0100*	2.62(0.38)
PI-1	98.2(22.1)	134.4(30.21)	1.47(0.06)	0.61(0.02)	0.0130	3.24(0.47)
WI-1	153.2(34.4)	169.7(38.2)	0.22(0.01)	0.02(0.001)	0.0023	4.27(0.62)

PI-2	99.0(22.3)	189.6(42.6)	14.40(0.57)	1.38(0.054)	0.0091	4.34(0.63)
WI-2	256.2(57.6)	269.3(60.5)	0.43(0.02)	0.09(0.004)	0.0018	6.62(0.96)

<sup>a</sup>Measured at  $\sim (0.025 - 0.050)$  mm crack width at interface, <sup>b</sup>Measured at peak load, \*Maximum recorded reading of strain gauge (at 89 kN)

All the specimens had a linear force versus slip relationship until cracking was observed at the interface. The resistance at this shear load was provided by cohesive bond between NSC and UHPC concrete particles. Specimens with WI interface roughness had a higher cracking load than PI specimen due to higher interface roughness. After the initiation of interface crack, the crack widened with application of additional load, subjecting the interface reinforcement to higher tensile strains. However, in specimens having smooth interface texture, significant slip was observed immediately after formation of interface crack. This behavior can be explained using shear friction theory; as specimen with smooth interface will have lower clamping force across the interface due to low coefficient of friction.

At peak load, WI specimen with interface reinforcement experienced lower slip and crack width compared to PI and SM specimen with interface reinforcement (see Table 3). At peak capacity, the interface reinforcement of specimen WI-2 had strain value of 1800 micro strain while the interface reinforcement of specimen PI-2 had strain value of 9100 micro strain. In contrary to traditional shear friction theory, the peak capacity with doubling the shear reinforcement was only increased by 1.6 and 1.4 times for WI (5 mm roughness) and PI (2 mm roughness) specimens. After reaching peak load, specimen with higher roughness and interface shear reinforcement (WI-1 and WI-2) resisted nearly 2/3 of peak shear load and were able to sustain higher slip values before failing. Specimen PI-2 underwent higher slip at peak load compared to WI-2 and failed immediately. Specimen PI-1 sustained additional slip and failed after shearing of the interface reinforcement. Specimen SM-1-A and SM-1-B formed a loading plateau as shown in Figure 2c and failed immediately after reaching peak load. WI-1 and WI-2 specimen showed superior post peak performance owing to lower slip, cracking and tensile strain in interface reinforcement at peak load. Specimens having no interface reinforcement failed immediately after beginning to slip at the interface.

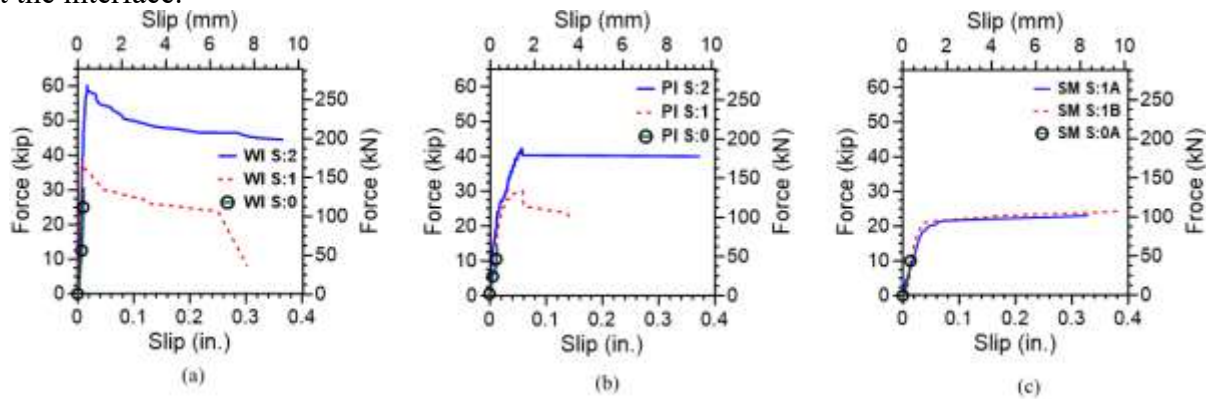
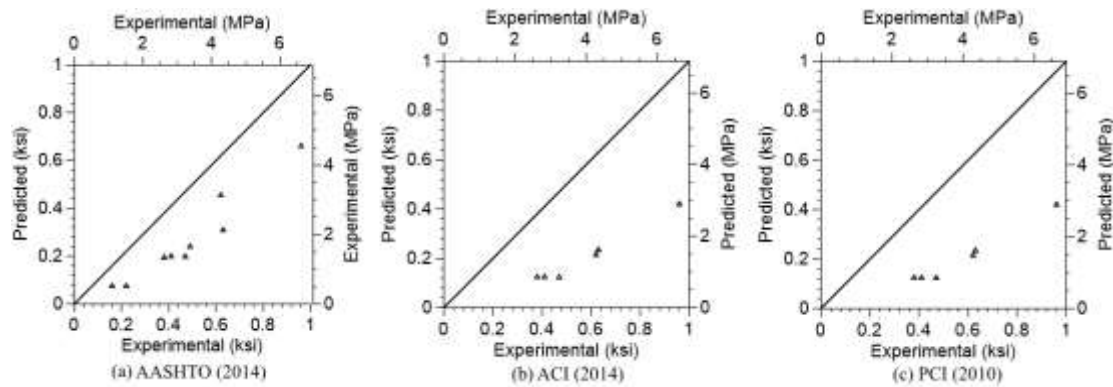


Figure 2 Force vs slip relationship across different interface roughness: (a) Wisla; (b) Parana; (c) Smooth



**Figure 3 Comparison of predicted and experimental strength**

Figure 3 shows comparison of predicted nominal strength using code provisions in Table 1 with experimentally obtained strength. The results indicate that code provisions are conservative in estimating interface shear capacity.

#### 4. Reliability Analysis

The reliability analysis was carried out to calculate reliability index of Interface Shear Transfer (IST) model, used in current AASHTO LRFD (2017) specifications for NSC-UHPC composites. According to section 5.7.4 of AASHTO LRFD, the factored interface shear resistance except for extreme event load combinations is determined by:

$$V_{ri} = \phi V_{ni} \quad (3)$$

where,  $V_{ni}$  = nominal interface shear resistance as defined in Table 1,  $\phi$  = resistance factor for shear specified in Article 5.5.4.2.

##### 4.1. Resistance Model

As per the AASHTO LRFD (2017) specifications the limit state factored load combination for horizontal shear resistance at interface of a bridge deck and bridge girder is Strength-I load combination. So, replacing ' $V_{ri}$ ' in equation 3 with Strength-I load combination and rearranging:

$$V_{ni} = \frac{\gamma_{DC} DC + \gamma_{DW} DW + \gamma_{LL} (LL + IM)}{\phi} \quad (4)$$

where,  $\gamma_{DC}$  = load factor of DC=1.25, DC= dead load from the weight of structural components and non-structural attachments,  $\gamma_{DW}$ = load factor of DW=1.50, DW= dead load from the weight of the wearing surface,  $\gamma_{LL}$ = load factor LL=1.75, LL= live load from the forces from moving vehicles in the bridge,  $IM$ = impact load from the forces produced by moving vehicles on the bridge. (Load factor values are for AASHTO LRFD Strength-I load combination)

The resistance model can be written as:

$$R = V_{ni} MFP \quad (5)$$

where, M = material factor (accounts for variation in material properties), F = fabrication factor (accounts for variation in fabrication/construction process) and P = professional factor (accounts for accuracy of design equations in predicting actual behavior).

The mean  $m_r$  and coefficient of variation  $COV_r$  values of the resistance model is given by the following equations:

$$m_R = V_{ni} \lambda_M \lambda_F \lambda_P \quad (6)$$

In equation (6),  $\lambda_M$  = bias factor of M,  $\lambda_F$  = bias factor of F and  $\lambda_P$  = bias factor of P

$$COV_R = \sqrt{COV_M^2 + COV_F^2 + COV_P^2} \quad (7)$$

where,  $COV_M$  = coefficient of variation of M,  $COV_F$  = coefficient of variation of F,  $COV_P$  = coefficient of variation of P.

The bias factor and COV for material and fabrication factor is taken from literature (Nowak et al. 2005). The bias factor and COV for professional factor was calculated by comparing the interface shear transfer prediction using AASHTO LRFD (2017) provision with the experimental results found in literature. A total of 80 push off test specimens across four research group was taken into account for calculation of professional bias factor. While calculating the professional factor, the test specimen were categorized according to weight of concrete and interface preparation to obtain reliability indices for different combinations. Specimens without interface reinforcement were included in calculation of professional factor. Specimens tested by Jang et al. with horizontal grooves greater than 20 mm. (0.79 in.) were neglected. Table 4 provides statistical parameters of resistance model.

**Table 4 Statistical parameters of resistance model**

Concrete Weight	Interface Preparation	Research Group	Nos. of Specimen	P		M		F	
				$\lambda$	cov	$\lambda$	cov	$\lambda$	cov
Normal Weight	Rough	Crane (5), Jang et al. (5), Sharma et al. (3)	13	2.32	0.31	1.22	0.12	1.01	0.04
	Smooth	Crane (21), Jang et al. (2), Sharma et al. (6)	29	2.55	0.41				
	Monolithic	Crane (12), Jang et al. (2)	14	4.80	0.36				
Light Weight	Rough	Banta (6)	6	1.14	0.32				
	Smooth	Banta (18)	18	1.73	0.30				
	Monolithic	N/A	N/A						

#### 4.2. Load Model

The load model Q is given by the following equation:

$$Q = DC + DW + LL + IM \quad (8)$$

The mean  $m_Q$  and coefficient of variation  $COV_Q$  values of the load model are given below:

$$m_Q = \lambda_{DC} DC + \lambda_{DW} DW + \lambda_{LL+IM} (LL + IM) \quad (9)$$

where,  $\lambda_{DC}$  = bias factor for DC,  $\lambda_{DW}$  = bias factor for DW,  $\lambda_{LL+IM}$  = bias factor for LL+IM

$$COV_Q = \sqrt{COV_{DC}^2 + COV_{DW}^2 + COV_{LL+IM}^2} \quad (10)$$

where,  $COV_{DC}$  = bias factor for DC,  $COV_{DW}$  = bias factor for DW,  $COV_{LL+IM}$  = bias factor for LL+IM.

Table 5 provides the statistical parameters for the load model (Nowak A. 1999).

**Table 5 Statistical Parameters of Load Model**

Statistical Parameter	Bias Factor( $\lambda$ )	Coefficient of Variation (COV)
DC	1.05	0.1
DW	1.05	0.25
LL+IM	1.28	0.18

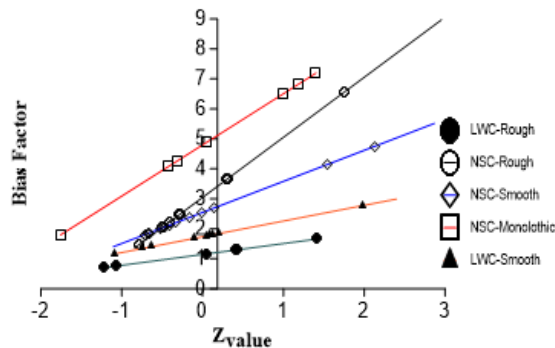


**Figure 4 Normality Check for Professional Factor**

#### 4.3. Normality of parameters in load and resistance model

Previous reliability studies in the literature have established all the parameters related to load model to be normally distributed (Nowak et al., 2005). In the resistance model, material and fabrication parameters have also been proven to be normally distributed (Soltani, 2018). To check for normality of the professional factor, the standard normal variable  $Z_{value}$  is calculated using equation 12 below and plotted against bias factor, in Figure 4. As shown in the Figure 4, the resulting line is straight line, indicating the distribution for the professional factor can be considered to be normal distribution.

$$Z_{value} = \frac{\left(\frac{V_{exp}}{V_n}\right)_i - Avg\left(\frac{V_{exp}}{V_n}\right)}{SD\left(\frac{V_{exp}}{V_n}\right)} \quad (11)$$

where,  $V_{exp}$  = measured experimental IST strength,  $V_n$  = predicted nominal IST strength,  $Avg\left(\frac{V_{exp}}{V_n}\right)$  = mean value of the strength ratio,  $SD\left(\frac{V_{exp}}{V_n}\right)$  = standard deviation of the strength ratios.

#### 4.4. Reliability Analysis of AASHTO IST Model

As the parameters related to load and resistance model are established to be normally distributed, equation 2 was used to calculate the reliability index. Reliability indices for multiple categories listed in Table 4 were calculated across different load ratios calculated using equation 12 and 13.

$$DR = \frac{DC}{DC+DW} \quad (12)$$

$$LR = \frac{LL+IM}{DC+DW+(LL+IM)} \quad (13)$$

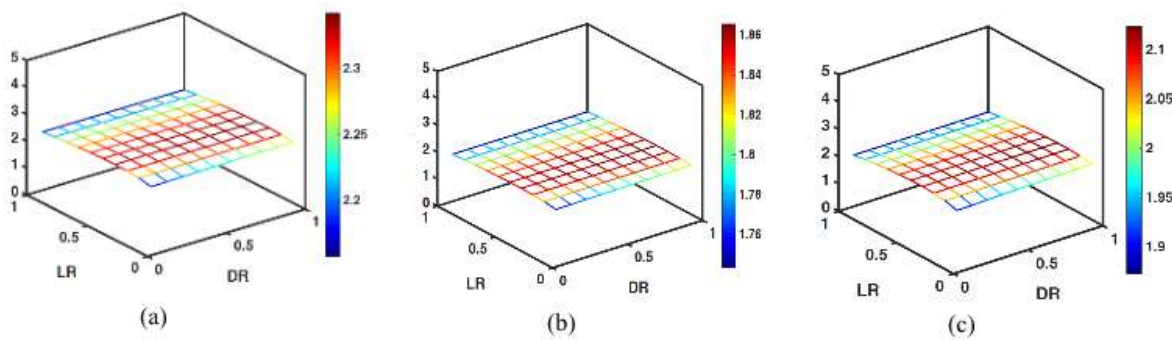


**Figure 5 Distribution of reliability indices: (a) NWC-Rough interface (b) NWC-Smooth interface (c) LWC-Smooth interface**

The reliability indices calculated for different ranges of DR (0 to 1) and LR (0 to 1) are shown in Figure 5. The average reliability indices were NWC-Rough (2.3), NWC-Smooth (1.8), NWC-Monolithic (2.3) LWC-Rough (1.8) and LWC-Smooth (2.0). The distribution of reliability indices across different load ratio was similar for all surface preparation.

Due to limited number of tests available on NSC-UHPC interface in the literature; a definitive assertion could not be made from the obtained reliability indices. However, the reliability indices obtained from past reliability studies on NSC-NSC interface were also below target reliability index of 3.5 (Soltani 2018), (Lang 2011). In NSC-UHPC interface, the predictions using AASHTO LRFD provisions were conservative but inconsistent when compared with experimental results. This is reflected in higher COV values for professional factor (0.3-0.41) compared to that of material factor (0.12) and fabrication factor (0.04) as shown in Table 4. The higher COV values from professional factor increases COV and the standard deviation ( $\sigma_R$ ) for the resistance model (see eq. 7). From equation 2, it is clear that reliability indices decreases with increment in  $\sigma_R$ . To improve reliability indices, the AASHTO LRFD IST model should be further improved to predict experimental results with higher accuracy. This will decrease COV for professional factor and shall lead to higher reliability indices.

## 5. Conclusions

The experimental results showed adequate NSC-UHPC interface bond strength across all interface roughness and reinforcement distribution. The interface bond strength increased with increase in roughness and interface reinforcement. However, the increase in capacity was not linear with the amount of shear reinforcement across the interface. Also, at peak capacity, the strains in interface reinforcement were lower for specimen with higher roughness compared to specimen with lower interface roughness. Current code provisions were found to be conservative in predicting the interface shear capacity of NSC-UHPC interface. The reliability indices calculated based on AASHTO LRFD IST model for NSC-UHPC interface were short of target reliability index of 3.5, due to high COV of professional factor. An improved IST model with increased accuracy in predicting interface shear strength will aid in improving the reliability indices.

## 6. Acknowledgments

The study reported in this paper is partly supported by the National Science Foundation through the Engineering for Natural Hazards (ENH) program (grant number 1662963). Any opinions, findings, and

conclusions expressed in this paper are those of the authors, and do not necessarily represent those of the sponsor.

## 7. References

American Association of State Highway and Transportation Officials(AASHTO), *AASHTO LRFD Bridge Design Specifications, 7th ed.* , AASHTO ,Washington, DC, 2014.

Aaleti, S. and Sritharan, S., " Investigation of a suitable shear friction interface between UHPC and normal strength concrete for brige deck applications," Bridge Engineering Center, Iowa State University, Report no. InTrans Project 10-379, Ames, Iowa, 2017.

American Concrete Institute (ACI)., "Building Code Requirements for Structural Concrete (ACI 318-14)," Farmington Hills, MI, 2014.

American Society of Civil Engineers (ASCE). "Bridges, 2017 Infrastructure Report Card." Available at <https://www.infrastructurereportcard.org/wp-content/uploads/2017/01/Bridges-Final.pdf> [Cited June 10, 2017].

Banta, Timothy E.," Horizontal shear transfer between ultra high performance concrete and lightweight concrete", MS Thesis, Virginia Polytechnic Institute and State University, Blacksburg, Virginia, 2005.

Birkeland, P. W. and Birkeland, H.W., "Connection in precast concrete connections," *Journal of the American Concrete Institute* , Vol. 63(3), 1966 , pp. 345-368.

Crane, C.K., "Shear and shear friction of ultra-high performance concrete bridge griders," Phd Thesis, Georgia Institute of Technology, Atlanta, Georgia, 2010.

Jang, H., Lee, H.; Cho, K. and Kim, J., "Experimental study on shear performance of plain construction joints integrated with ultra-high performance concrete," *Construction and Building Materials*, Vol. 152, 2017, pp. 16-23.

Lang, Maria., "Analysis of the AASHTO LRFD Horizontal Shear Strength Equation," MS Thesis, Virginia Polytechnic Institue and State University, Blacksburg, VA, 2011.

Munoz, Miguel A.C., et al., "Bond Performance between Ultrahigh-Performance Concrete and Normal-Strength Concrete." *J. Mater. Civ. Eng., American Society of Civil Engineers*, Vol. 26, No. 8, 2014.

Nowak, A.S. et al., "Reliability-based Calibration for Structural Concrete," Department of Civil Engineering, University of Nebraska, Lincoln, NE, 2005.

Nowak, A.S. , "Calibration of LRFD Bridge Design Code." NCHRP (National Cooperative Highway Research Project) Report No. 368, Transportation Research Board, Washington, DC, 1999.

Nowak, A.S. and Collins, K.R., "Reliability of Structures," McGraw Hill, Singapore, 2000.

Precast/Prestressed Concrete Institute (PCI). "PCI Design Handbook," , PCI, Chicago, IL ,2010.

Santos, P.M.D. and Julio E.N.B.S., "Interface shear transfer on composite concrete members," *Structural Journal*, 2014, pp 113-122.

Sarkar, Jayeeta, "Characterization of the Bond Strength between Ultra High Performance Concrete Bridge Deck Overlays and Concrete Substrates." MS Thesis, Michigan Tech. University, 2010.

Soltani, M., "Reliability analyses of interface shear transfer in AASHTO LRFD specifications model and an alternative model." *PCI Journal*, Vol. 63, No. 5, 2018, pp. 36-50.